Sakarya University Journal of Science

ISSN 1301-4048 | e-ISSN 2147-835X | Period Bimonthly | Founded: 1997 | Publisher Sakarya University | http://www.saujs.sakarya.edu.tr/

Title: On the Analysis of Secrecy Outage Probability Using Average Channel Capacity

Authors: Ferkan Yılmaz

Recieved: 2019-12-06 20:01:32

Accepted: 2019-12-26 15:16:16

Article Type: Research Article
Volume: 24
Issue: 1
Month: February
Year: 2020
Pages: 248-256

Sakarya University Journal of Science 24(1), 248-256, 2020

SAKARYA UNIVERSITY

On the Analysis of Secrecy Outage Probability Using Average Channel Capacity

Ferkan YILMAZ [*1]

Abstract

In this article, we analyze the outage probability of physically secure wireless signal transmission in fading environments where both primary and eavesdropper channels are subject to generalized fading. We propose a novel approach using the average channel capacity of the primary channel and that of the eavesdropper channel to the outage probability of physically secure wireless signaling.

Keywords: Average channel capacity, secrecy outage probability, performance analysis, physical layer security.

1. INTRODUCTION

In wireless communication systems, information transmissions are inherently inclined to eavesdropping due to the broadcast essence of wireless channels. In this context, with the compelling concern of providing secure wireless communications, physical layer security, as an alternative to conventional cryptographic approaches, becomes an important issue that has attracted so much attention from theoreticians, practitioners, and researchers in the literature. Further, it certainly takes advantage of the physical characteristics (such as fading, noise, and diversity) of radio links to sustain secure communications. Cutting-edge studies on physical-layer security [1]–[4] carried on a primary wiretap channel where a legitimate user (say Alice) communicates with the intended receiver (say Bob) in the presence of an eavesdropper (say Eve), where all nodes are each equipped with one antenna. In this model, for the primary channel (from Alice to Bob), the maximal achievable rate without allowing Eve to obtain any information is termed secrecy capacity. In [1], Wyner showed that, even if Eve's channel is worse than Bob's one, it is possible to have nonzero secrecy capacity. Wyner's work was first extended in [2] to a non-degraded channel and then generalized in [3] to determine the secrecy capacity for a wiretap channel with additive white Gaussian noise (AWGN). Also, in [4], secrecy outage probability (SOP), sometimes called secure outage probability, was introduced as a secrecy performance metric over fading channels. In the literature, there are various researches and

[*] Corresponding E-mail: ferkan@yildiz.edu.tr

[1] Yıldız Technical University (YTU), Faculty of Electrical and Electronics Engineering, Computer Eng. Department, Istanbul TURKEY. ORCID: https://orcid.org/0000-0001-6502-8280

studies concerning the analysis of the secrecy performance in the single-input single-output (SISO) system where information is transmitted from Alice to Bob while Eve over-hears it over fading channels [5]–[17]. To the best of our knowledge, all the studies available in the literature [1]–[17] accomplish the SOP analysis using the statistical characterization of signal-to-noise ratios (SNR) of wireless links, that is widely described with the aid of probability density function (PDF), cumulative distribution function (CDF), moment-generating function (MGF), and higher-order moments.

In this article, to achieve the SOP analysis, we propose a novel approach using average channel capacity (ACC) performance of wireless links rather than using the PDF, CDF, MGF, and higher-order moments of their SNR distributions. In other words, without need the statistical characterization of SNR distributions, we present how to obtain the SOP from the averaged statistics that are the ACC performances of the primary channel and the eavesdropper channel.

The structure of this article is organized as follows. Section 2 describes the system model of interest. Section 3 presents an exact analysis of SOP in terms of ACC performance. Section 4 provides the numerical results of our analysis, followed by the conclusion given in the last section.

2. SYSTEM MODEL

Let us consider two nodes, say Alice (transmitter) and Bob (receiver), that Alice transmits confidential information to Bob over a wireless channel within the presence of an eavesdropper, say Eve, that secretly observes their transmission signaling [1]. To be realistic, we consider a silent eavesdropping scenario where Alice does not have the channel state information (CSI) of the Alice−Eve wireless link. In this scenario, perfect security of transmission from Alice to Bob cannot be guaranteed [1]. The instantaneous secrecy capacity, i.e., the instantaneous capacity of the secrecy in the primary link between Alice and Bob, is simply defined as [1]–[4]

$$C_S = \max(C_B - C_E, 0), \tag{1}$$

where $C_B = \log(1+\gamma_B)$ and $C_E = \log(1+\gamma_E)$ denote the instantaneous channel capacity (CC) of the Alice-Bob and Alice-Eve wireless channels, respectively. Furthermore, γ_B and γ_E denotes the instantaneous SNRs at Bob and Eve receivers, respectively, and they are, without loss of generality, assumed to be mutually independent. In (1), $\max(x,y)$ yields x if $x \geq y$, or otherwise y.

3. SECRECY OUTAGE PROBABILITY

In accordance with Section 2, the ACC of primary channel and the ACC of eavesdropper channels are obtained as $C_{avg}^{B}(\bar{\gamma}) = \mathbb{E}[C_B]$ and $C_{avg}^{E}(\bar{\gamma}) = \mathbb{E}[C_E]$, respectively, where $\mathbb{E}[\cdot]$ denotes the expectation operator. With the aid of their definitions, they are rewritten as

$$C_{avg}^{B}(\bar{\gamma}) = \mathbb{E}[\log(1+\gamma_B)], \tag{2}$$

$$C_{avg}^{E}(\bar{\gamma}) = \mathbb{E}[\log(1+\gamma_E)], \tag{3}$$

respectively, for an average SNR $\bar{\gamma}$, Thus, for a certain SNR threshold γ_{th} , their outage probabilities (OPs), i.e., $P_{out}^{B}(\gamma_{th}|\bar{\gamma}) = \Pr(\gamma_B \leq \gamma_{th})$ and $P_{out}^{E}(\gamma_{th}|\bar{\gamma}) = \Pr(\gamma_E \leq \gamma_{th})$ are respectively

$$P_{out}^{B}(\gamma_{th};\bar{\gamma}) = \mathbb{E}[\theta(\gamma_{th}-\gamma_B)], \tag{4}$$

$$P_{out}^{E}(\gamma_{th};\bar{\gamma}) = \mathbb{E}[\theta(\gamma_{th}-\gamma_E)], \tag{5}$$

where $\theta(\cdot)$ denotes the Heaviside's theta function [18, Eq. (1.8.3)], [19, Eq. (14.05.07.0002.01)], that is defined as

$$\theta(C_{th}-C_s) = \begin{cases} 1, & \text{if } C_{th} > C_s, \\ 1/2, & \text{if } C_{th} = C_s, \\ 0, & \text{if } C_{th} < C_s. \end{cases} \tag{6}$$

In addition, the SOP is widely used as an indicator for that secure transmission from Alice to Bob cannot be guaranteed. For a certain threshold C_{th}, the SOP is defined as the probability of that the distribution of secrecy capacity is less than or equal to C_{th}, and it is written as

$$C_{out}^{S}(C_{th};\bar{\gamma}_B,\bar{\gamma}_E) = \Pr(C_s \leq C_{th}), \tag{7a}$$

$$= \mathbb{E}[\theta(C_{th}-C_s)], \tag{7b}$$

where $\bar{\gamma}_B$ and $\bar{\gamma}_E$ denotes the average SNRs of the Alice-Bob and Alice-Eve wireless channels, respectively (i.e., $\bar{\gamma}_B = \mathbb{E}[\gamma_B]$ and $\bar{\gamma}_E = \mathbb{E}[\gamma_E]$). Further, as seen in (7a), the analysis of SOP, i.e., the analysis of $C_{out}(C_{th}; \bar{\gamma}_B, \bar{\gamma}_E)$ requires the statistical characterizations of both γ_B and γ_E. In the evaluation of OP and SOP, Heaviside's theta function $\theta(x-y)$ exhibits a discontinuity at $x = y$. This discontinuity prevents obtaining closed-form results. It is therefore usually replaced by the limit representation of smooth and nonlinear functions [19, Eq. (14. 05.09.0001) and others therein]. However, we introduce in Theorem 1 an alternative exact form of $\theta(x-y)$ which has not been reported in the literature so far. The novelty of this alternative form is being an exact expression obtained neither by the limit of a function nor a sequence of functions with convergence.

Theorem 1. *An exact and closed-form representation of* $\theta(x-y)$ *is given by*

$$\theta(x-y) = \frac{1}{\pi}\Im\left\{\log\left(1-\frac{x}{y}\right)\right\}, \tag{8}$$

for $x \in \mathbb{R}^+$ *and* $y \in \mathbb{R}^+$, *where* $\Im\{\cdot\}$ *yields the imaginary part of its argument.*

Proof: In accordance with [20, Theorem 5], the quasi-increasing property of $\theta(x-1)$ (i.e., $\theta(x-1) \geq \theta(y-1)$ for $x \geq y$) allows a theoretical relation between $\theta(x-1)$ and $\log(1+x)$. In the context of [20, Theorem 4], the Lamperti's dilation spectrum (LDS) of $\log(1+x)$ can be obtained as

$$L(\omega, x) = \mathfrak{F}_\lambda\{\mathfrak{L}_{H,x}^{-1}\{\log(1+x)\}(\lambda)\}(\omega) \tag{9a}$$

$$= -x^{H+i\omega}\Gamma(H+i\omega)\Gamma(-H-i\omega) \tag{9b}$$

for the Hurst's exponent $0 < H < 1$, where $\mathfrak{L}_{H,x}^{-1}\{\cdot\}(\lambda)$ denotes the inverse Laperti's transformation defined in [20, Eq. (15)], and $\mathfrak{F}_\lambda\{\cdot\}(\omega)$ denotes the Fourier's transform with respect to $\lambda \in \mathbb{R}^+$. $\Gamma(\cdot)$ is the Gamma function [21, Eq. (6.5.3)]. Similarly, the LDS of $\theta(x-1)$ can be derived as

$$T(\omega, x) = \mathfrak{F}_\lambda\{\mathfrak{L}_{H,x}^{-1}\{\theta(x-1)\}(\lambda)\}(\omega), \tag{10a}$$

$$= -x^{H+i\omega}(H+i\omega)^{-1}, \tag{10b}$$

for the Hurst's exponent $0 < H < \infty$. Using [19, Eq. (06.05.16.0010.01)], the ratio of (10b) to (9b) is simplified to

$$\frac{T(\omega, x)}{L(\omega, x)} = -\frac{1}{\pi}\sin\big(\pi(H+i\omega)\big), \tag{11}$$

whose substitution into [19, Eq. (33)] yields

$$z(u) = \mathfrak{L}_{-(H+1),\lambda}\left\{u^{-(H+1)+i\omega} \times \mathfrak{F}_\omega^{-1}\left\{\frac{T(\omega, x)}{L(\omega, x)}\right\}(\lambda)\right\}(u), \tag{12a}$$

$$= \frac{1}{\pi}\Im\left\{\frac{1}{2\pi i}\int_{-H-i\infty}^{-H+i\infty} u^{s-1}e^{j\pi s}ds\right\}. \tag{12b}$$

Thus, referring to [19, Theorem 4], $\theta(x-1)$ can be rewritten in terms of $\log(1+x)$, that is $\theta(x-1) = \int_0^\infty z(u)\log(1+ux)\,du$, where putting (8b) results in

$$\theta(x-1) = \frac{1}{\pi}\Im\left\{\log(1-x)\right\}, \tag{13}$$

which is the first step of the proof. In the second step, with the aid of [19, (14.05.17.0001.01)], we can write $\theta(x-y) = \theta(x/y - 1)$, where inserting (13) yields (8), which proves Theorem 1. ■

With the results presented above, we show in the following that we need to have the next property of Heaviside's theta function to achieve the SOP analysis of the system model defined in Section 2.

Theorem 2. *Let* $f(x)$ *be a continuous and monotonic function over* $x \in \mathbb{R}^+$. *If* $f(x)$ *is increasing with respect to x (i.e.,* $\partial f(x)/\partial x \geq 0$*), then*

$$\theta(x-y) = \theta\big(f(x) - f(y)\big); \tag{14}$$

if decreasing (i.e., $\partial f(x)/\partial x < 0$*), then*

$$\theta(x-y) = \theta\big(f(y) - f(x)\big), \tag{15}$$

for any $x, y \in \mathbb{R}^+$.

Proof: The proof is obvious using the property that Heaviside's theta function is a quasi-monotonically increasing function. ■

With the aid of Theorem 1 and Theorem 2, we can show how to obtain the SOP of the system model, defined in Section 2, in terms of the ACC of the primary channel and the ACC of the eavesdropper channel, especially without the need for the statistical characterizations of the instantaneous SNRs γ_B and γ_E. Accordingly, we present this novel SOP analysis in the following theorem.

Theorem 3. *If the ACC of the primary channel and the ACC of the eavesdropper channel, i.e., $C_{avg}^{B}(\bar{\gamma})$ and $C_{avg}^{E}(\bar{\gamma})$ are known, then the SOP for a certain threshold C_{th}, i.e., $C_{out}^{S}(C_{th}|\bar{\gamma}_B,\bar{\gamma}_E)$ is given by*

$$C_{out}^{S}(C_{th};\bar{\gamma}_B,\bar{\gamma}_E) = 1 + \frac{1}{\pi^2}\int_0^\infty \Im\left\{C_{avg}^{B}\left(-\frac{\bar{\gamma}_B}{e^{C_{th}}(1+u)-1}\right)\right\} \times \Im\left\{\frac{\partial}{\partial u}C_{avg}^{E}\left(-\frac{\bar{\gamma}_E}{u}\right)\right\} du, \tag{18}$$

where $\bar{\gamma}_B$ and $\bar{\gamma}_E$ denote the average SNRs of the Alice-Bob and Alice-Eve channels, respectively.

Proof: As explained before, the SOP is defined as the probability that the achievable secrecy rate is less than a given secrecy code rate which is non-negative. With the aid of (1) and (7) and using $C_S = \max(C_B - C_E, 0) = (C_B - C_E)\theta(C_B - C_E)$, we rewrite the SOP as

$$C_{out}^{S}(C_{th};\bar{\gamma}_B,\bar{\gamma}_E) = \mathbb{E}[\theta(C_{th} - C_S)], \tag{19a}$$

$$= \mathbb{E}[\theta(C_{th} + C_E - C_B)], \tag{19b}$$

wherein substituting both $C_B = \log(1+\gamma_B)$ and $C_E = \log(1+\gamma_E)$ results in

$$C_{out}^{S}(C_{th};\bar{\gamma}_B,\bar{\gamma}_E) = \mathbb{E}[\theta(e^{C_{th}}(1+\gamma_E) - 1 - \gamma_B)]. \tag{20}$$

where the expectation operator $\mathbb{E}[\cdot]$ is achieved with respect to γ_B and γ_E. Note that the OP of the primary channel is given by $P_{out}^{B}(\gamma_{th};\bar{\gamma}_B) = \mathbb{E}[\theta(\gamma_{th} - \gamma_B)]$. Accordingly, and consequently, (19) is simplified to

$$C_{out}^{S}(C_{th};\bar{\gamma}_B,\bar{\gamma}_E) = \mathbb{E}[P_{out}^{B}(e^{C_{th}}(1+\gamma_E) - 1;\bar{\gamma}_B)]. \tag{21}$$

If the PDF of γ_E, i.e., $p_{\gamma_E}(\gamma;\bar{\gamma})$ is known and can be obtained as $p_{\gamma_E}(\gamma;\bar{\gamma}) = \partial P_{out}^{E}(\gamma;\bar{\gamma})/\partial\gamma$, then (21) can be readily computed as

$$C_{out}^{S}(C_{th};\bar{\gamma}_B,\bar{\gamma}_E) = \int_0^\infty P_{out}^{B}(e^{C_{th}}(1+\gamma) - 1;\bar{\gamma}_B) \times p_{\gamma_E}(\gamma;\bar{\gamma}_E)\, d\gamma. \tag{22a}$$

$$= \int_0^\infty P_{out}^{B}(e^{C_{th}}(1+\gamma) - 1;\bar{\gamma}_B) \times \left\{\frac{\partial}{\partial\gamma}P_{out}^{E}(\gamma;\bar{\gamma}_E)\right\} d\gamma. \tag{22b}$$

In accordance with the benightment of [20] and applying Theorem 1 on (4), we can alternatively evaluate the OP of Alice-Bob channel as follows

$$P_{out}^{B}(\gamma_{th};\bar{\gamma}_B) = 1 - \frac{1}{\pi}\Im\left\{\mathbb{E}\left[\log\left(1 - \frac{\gamma_B}{\gamma_{th}}\right)\right]\right\}, \tag{23a}$$

$$= 1 - \frac{1}{\pi}\Im\left\{C_{avg}^{B}\left(-\frac{\bar{\gamma}_B}{\gamma_{th}}\right)\right\}, \tag{23b}$$

It is worth mentioning that (23b) presents that the ACC of the primary (Alice-Bob) channel is sufficient to obtain its OP performance. Similarly, the ACC of the eavesdropper (Alice-Eve) channel is also enough and sufficient to obtain its OP performance, that is

$$P_{out}^{E}(\gamma_{th};\bar{\gamma}_E) = 1 - \frac{1}{\pi}\Im\left\{\mathbb{E}\left[\log\left(1 - \frac{\gamma_E}{\gamma_{th}}\right)\right]\right\}, \tag{24a}$$

$$= 1 - \frac{1}{\pi}\Im\left\{C_{avg}^{E}\left(-\frac{\bar{\gamma}_E}{\gamma_{th}}\right)\right\}. \tag{24b}$$

Finally, replacing both (23b) and (24) into (22b) and performing simple algebraic manipulations yields (18), which proves Theorem 3. ■

The resulting finite-range integration in (18) can be evaluated very accurately with only a few function samples using the Gauss-Chebyshev quadrature (GCQ) formula [22]. The computational performance of our new expression present itself as

$$C_{out}^{S}(C_{th};\bar{\gamma}_B,\bar{\gamma}_E) \approx 1 + \frac{1}{\pi^2}\sum_{n=1}^{N}\omega_n \Im\left\{C_{avg}^{B}\left(-\frac{\bar{\gamma}_B}{e^{C_{th}}(1+u_n)-1}\right)\right\}\Im\left\{\frac{\partial}{\partial u_n}C_{avg}^{E}\left(-\frac{\bar{\gamma}_E}{u_n}\right)\right\}, du, \quad (25)$$

a powerful tool for SOP analysis under a myriad of fading scenarios. Additionally, we can accurately estimate the SOP as in (25) on the top of the next page, which converges quickly, requiring only few terms for an accurate result. Moreover, the abscissas u_n and weights ω_n can be given in closed form [22, Eq. (9)] as follows

$$u_n = \tan\left(\frac{\pi}{4}\cos\left(\frac{2n-1}{2N}\pi\right)+\frac{\pi}{4}\right), \quad (26a)$$

$$\omega_n = \frac{\pi^2 \sin\left(\frac{2n-1}{2N}\pi\right)}{4N\cos^2\left(\frac{\pi}{4}\cos\left(\frac{2n-1}{2N}\pi\right)+\frac{\pi}{4}\right)}, \quad (26b)$$

respectively, where N is the truncation chosen as $N = 50$ to reach a high accuracy in calculations.

4. NUMERICAL RESULTS

In this section, we provide simulation results to check and validate the accuracy and completeness of our SOP analysis, proposed in the previous section. From the system design point of view, it is beneficial to have a general distribution whose versatility seems the most appropriate for the statistical characterization of fading channels. The extended generalized-K (EGK) distribution was proposed in [23], [24] as a very general one whose special cases, including those given in [24, Table 1], are widely used in the literature. The significance of EGK distribution in describing various fading/shadowing environments, as well as performance evaluations, have been presented in [23], [24]. Assuming the instantaneous SNR γ_B of the primary channel follows EGK distribution, we can write the PDF of γ_B as [24, Eq. (3)]

$$f_{\gamma_B}(\gamma;m,m_s,\xi,\xi_s) = \frac{\xi}{\Gamma(m_s)\Gamma(m)}\left(\frac{\beta_s\beta}{\bar{\gamma}}\right)^{m\xi} \times \gamma^{m\xi-1}\,\Gamma\left(m_s - m\frac{\xi}{\xi_s}, 0, \left(\frac{\beta_s\beta}{\bar{\gamma}}\right)^{m\xi}\gamma, \frac{\xi}{\xi_s}\right), \quad (27)$$

defined over $0 \leq \gamma < \infty$, wherein the parameters m $(0.5 \leq m < \infty)$ and ξ $(0.5 \leq \xi < \infty)$ denote the fading figure and shaping factors, respectively, while m_S $(0.5 \leq m_S < \infty)$ and ξ_S $(0.5 \leq \xi_S < \infty)$ denote the shadowing severity and shaping factors, respectively. The parameter $\bar{\gamma}$ is the average power (i.e., $\bar{\gamma} = \mathbb{E}[\gamma_B]$). Furthermore, β and β_s are expressed as $\beta = \Gamma(m+1/\xi)/\Gamma(m)$ and $\beta_s = \Gamma(m_s+1/\xi_s)/\Gamma(m_s)$, respectively, and $\Gamma(\alpha,x,b,\beta) = \int_x^\infty r^{\alpha-1}\exp\left(-r - br^{-\beta}\right)dr$ is the extended incomplete Gamma function with parameters $\alpha, b, \beta \in \mathbb{C}$ and $x \in \mathbb{R}^+$ [25, Eq. (6.2)]. With the aid of [23, Eq. (42)], [24, Eq. (14)], we can obtain the ACC of the primary channel as

$$C_{avg}^{B}(\bar{\gamma}) = \frac{1}{\Gamma(m)\Gamma(m_s)} \times \mathrm{H}_{2,4}^{4,1}\left[\frac{\beta_s\beta}{\bar{\gamma}}\middle| \begin{matrix}(0,1),(1,1)\\ (m,1/\xi),(m_s,1/\xi_s),(0,1),(0,1)\end{matrix}\right], \quad (28)$$

where $\mathrm{H}_{p,q}^{m,n}[\cdot]$ is the Fox's H function [26], [27]. Setting the shaping factors $\xi = \xi_s = 1$ and then using [28, Eq. (8.3.21)], we readily reduce (28) to [23, Eq. (43)], [24, Eq. (15)]

$$C_{avg}^{B}(\bar{\gamma}) = \frac{1}{\Gamma(m)\Gamma(m_s)}\mathrm{G}_{2,4}^{4,1}\left[\frac{mm_s}{\bar{\gamma}}\middle| \begin{matrix}0,1\\ m,m_s,0,0\end{matrix}\right], \quad (29)$$

where $\mathrm{G}_{p,q}^{m,n}[\cdot]$ is the Meijer's G function [28, Eq. (8.3.22)]. Setting the shaping and figure factors of shadowing as $\xi_s = 1$ and as, $m_s \to \infty$ and using [21, Eq. (6.1.46)], we reduce (28) to the ACC of Nakagami-m fading channels, that is [29, Eq. (3)]

$$C_{avg}^{B}(\bar{\gamma}) = \frac{1}{\Gamma(m)}\mathrm{G}_{2,3}^{3,1}\left[\frac{m}{\bar{\gamma}}\middle| \begin{matrix}0,1\\ m,0,0\end{matrix}\right]. \quad (30)$$

Similarly, assuming the instantaneous SNR γ_E of the eavesdropper channel follows EGK distribution, we can write its ACC performance in accordance with (28), that is

$$C_{avg}^{E}(\bar{\gamma}) = \frac{1}{\Gamma(n)\Gamma(n_s)} \times \mathrm{H}_{2,4}^{4,1}\left[\frac{B_sB}{\bar{\gamma}}\middle| \begin{matrix}(0,1),(1,1)\\ (n,1/\phi),(n_s,1/\phi_s),(0,1),(0,1)\end{matrix}\right], \quad (31)$$

where the parameters $n, n_s, \phi, \phi_s, B, B_s$ have the same meaning and definition of $m, m_s, \xi, \xi_s, \beta, \beta_s$, respectively. The special cases of (31) are similar to that of

$$C_{out}^{S}(C_{th};\bar{\gamma}_B,\bar{\gamma}_E)=\frac{1}{\Gamma(m)\Gamma(m_s)\Gamma(n)\Gamma(n_s)}\int_0^\infty\frac{1}{u}\,\mathrm{H}_{1,3}^{3,0}\left[\frac{\beta_s\beta}{\bar{\gamma}}(e^{C_{th}}(1+u)-1)\middle|\begin{matrix}(1,1)\\(m,1/\xi),(m_s,1/\xi_s),(0,1)\end{matrix}\right]\times\mathrm{H}_{0,2}^{2,0}\left[\frac{B_sB}{\bar{\gamma}}u\middle|\begin{matrix}\overline{}\\(n,1/\phi),(n_s,1/\phi_s)\end{matrix}\right]du, \tag{35}$$

(28) for certain values of n, n_s, ϕ, ϕ_s. With the aid of Theorem 3 using (28) and (31), we obtain the SOP for a certain rate threshold C_{th} as follows

$$C_{out}^{S}(C_{th};\bar{\gamma}_B,\bar{\gamma}_E)=1+\frac{1}{\pi^2}\times\int_0^\infty\Im\left\{C_{avg}^{B}\left(-\frac{\bar{\gamma}_B}{e^{C_{th}}(1+u)-1}\right)\right\}\times\Im\left\{\frac{\partial}{\partial u}C_{avg}^{E}\left(-\frac{\bar{\gamma}_E}{u}\right)\right\}du, \tag{32}$$

where, using [20, Theorem 9], $\Im\{C_{avg}^{B}(-\bar{\gamma}_B/u)\}$ and $\Im\{(\partial/\partial u)C_{avg}^{E}(-\bar{\gamma}_E/u)\}$ are readily reduced to the π times of the complementary CDF of the SNR γ_E of the eavesdropper channel [24, Eq. (14)] and the $-\pi$ times of the PDF of the SNR γ_E of the eavesdropper channel [23, Eq. (5)], respectively, that are

$$\Im\left\{C_{avg}^{B}\left(-\frac{\bar{\gamma}}{u}\right)\right\}=\pi\left(1-\frac{1}{\Gamma(m)\Gamma(m_s)}\times\mathrm{H}_{1,3}^{3,0}\left[\frac{\beta_s\beta}{\bar{\gamma}}u\middle|\begin{matrix}(1,1)\\\left(m,\frac{1}{\xi}\right),\left(m_s,\frac{1}{\xi_s}\right),(0,1)\end{matrix}\right]\right), \tag{33}$$

$$\Im\left\{\frac{\partial}{\partial u}C_{avg}^{E}\left(-\frac{\bar{\gamma}}{u}\right)\right\}=-\frac{\pi}{\Gamma(n)\Gamma(n_s)\,u}\times\mathrm{H}_{0,2}^{2,0}\left[\frac{B_sB}{\bar{\gamma}}u\middle|\begin{matrix}\overline{}\\\left(n,\frac{1}{\phi}\right),\left(n_s,\frac{1}{\phi_s}\right)\end{matrix}\right], \tag{34}$$

as expected, where – the empty set of parameters. Consequently, substituting (33) and (34) into (32), we obtain the SOP as (35) on the top of this page, whose numerical evaluations have been exactly calculated and compared with the simulation-based results for different fading environment parameters $\{m, m_s, \xi, \xi_s$ $n, n_s, \phi, \phi_s\}$ in the Figure 1, wherein numerical and simulation-based results are in perfect agreement. Further-more, in Figure 1, it is worth noticing the secrecy of the primary channel decreases when the SNR of the eavesdropper channel increases (i.e., when Eve gets closer to Alice). The other important observation is that the secrecy strictly depends on the SNR of the primary channel. In particular, the secrecy is always possible if and only if the SNR of the primary (Alice-Bob) channel is higher than that of the eavesdropper channel. In other words, in order to provide secrecy for the primary channel, Bob has to be spatially much closer to Alice than Eve does.

In Figure 2, we investigate how the diversity orders (fading figures) of the primary and eavesdropper channels, i.e., the number of antennas on Bob's and Eve's receivers affect the SOP performance when these channels have the same average SNR (i.e., Bob and Eve are spatially in same distance to Alice). Within that context, we observe that the secrecy of the primary channel increases when the number of antennas on Bob's receiver increases. Of course, while the number of antennas on Eve's receiver increases, the secrecy of the primary channel decreases. How-ever, the secrecy is more susceptible to the diversity order of the primary channel (i.e., the number of antennas on Bob's receiver) rather than that of the eavesdropper channel.

5. CONCLUSION

In this article, we provide a novel approach using ACC of primary and eavesdropper channels to achieve the SOP analysis in fading environments. Our analytical and closed-form results demonstrate that the ACC is enough and sufficient for SOP analysis. The analytical formulation of SOP analysis is illustrated for EGK fading environments, and accordingly some simulations have been carried out. The results show that numerical results and simulation results are in perfect agreement.

6. ACKNOWLEDGMENTS

The author would like to thank the editor and anonymous reviewers for their constructive comments.

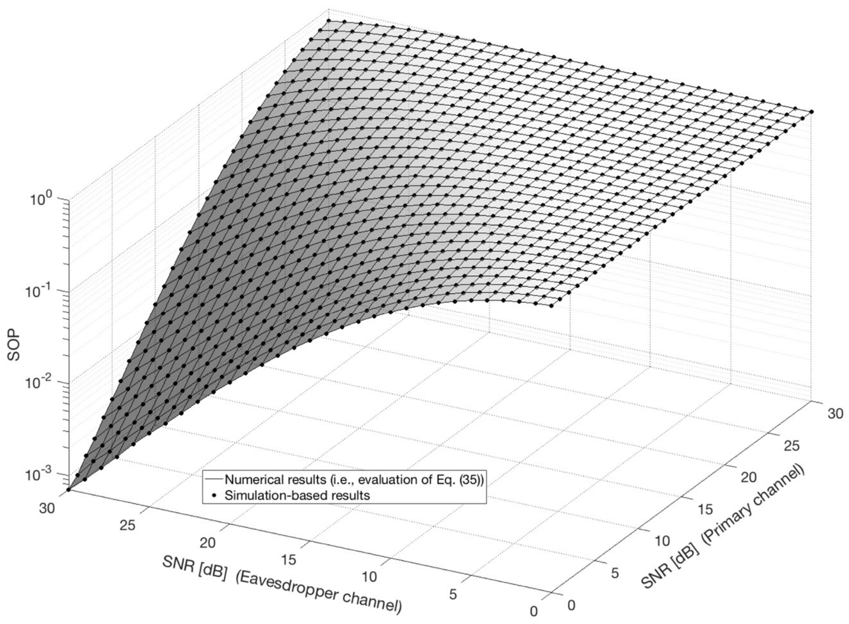

Figure 1. For the rate threshold $\boldsymbol{C_{th}} = \mathbf{1}$ nats/sn/Hz , the SOP performance in EGK fading environments, where the parameters of the primary channel are $\boldsymbol{m} = \boldsymbol{m_s} = \mathbf{2}$ and $\boldsymbol{\xi} = \boldsymbol{\xi_s} = \mathbf{1}$, and the parameters of the eavesdropper channel are $\boldsymbol{n} = \boldsymbol{n_s} = \mathbf{2}$ and $\boldsymbol{\phi} = \boldsymbol{\phi_s} = \mathbf{1}$

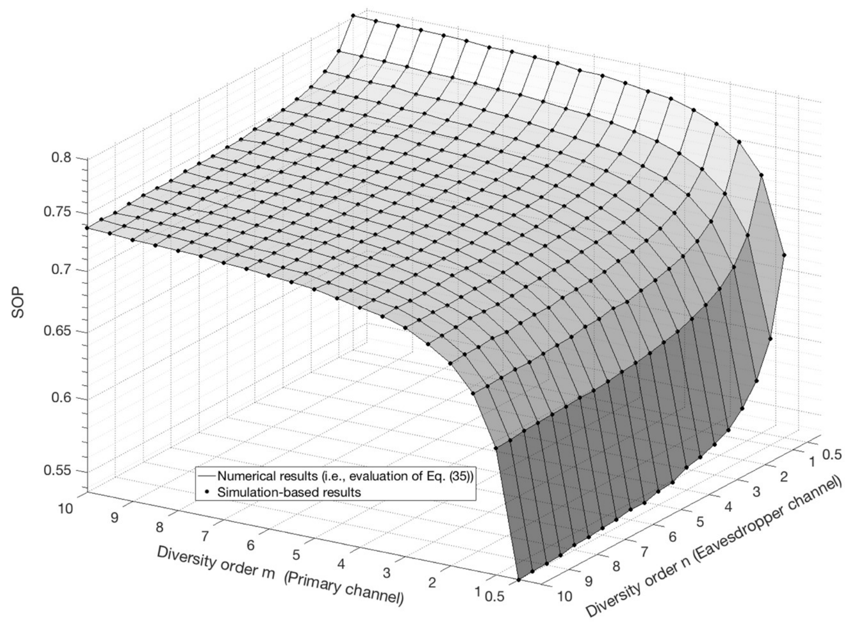

Figure 2. For the rate threshold $C_{th} = 1$ nats/sn/Hz , the SOP performance in EGK fading environments, where the average SNRs of the primary and eavesdropper channels are the same (i.e., $\overline{\gamma}_B = \overline{\gamma}_E = 15$ dB). Further, the other parameters are $m_s = n_s = 2$ and $\xi = \xi_s = \phi = \phi_s = 1$.

7. REFERENCES

[1] A. D. Wyner, “The wire-tap channel,” *Bell System Technical Journal*, vol. 54, no. 8, pp. 1355–1387, 1975.

[2] I. Csiszár, and J. Körner, “Broadcast channels with confidential messages,” *IEEE Transactions on Information Theory*, vol. 24, no. 3, pp. 339–348, 1978.

[3] S. Leung-Yan-Cheong, and M. Hellman. “The Gaussian wire-tap channel,” *IEEE Transactions on Information Theory, vol.* 24, no. 4, pp. 451–456, (1978).

[4] M. Bloch, J. Barros, M. R. Rodrigues, and S. W. McLaughlin, “Wireless information-theoretic security,” *IEEE Transactions on Information Theory*, vol. 54, no. 6, pp. 2515–2534, 2008.

[5] M. Z. I. Sarkar, T. Ratnarajah, and M. Sellathurai, “Secrecy capacity of Nakagami-*m* fading wireless channels in the presence of multiple eavesdroppers,” *in* Conference Record of the Forty-Third Asilomar Conference on Signals, Systems and Computers, Pacific Grove, California, USA, Nov. 2009, pp. 829–833.

[6] X. Liu, “Outage probability of secrecy capacity over correlated log–normal fading channels,” *IEEE Communications Letters*, vol. 17, no. 2, pp. 289–292, Feb. 2013.

[7] D.-B. Ha, T. Q. Duong, D.-D. Tran, H.–J. Zepernick, and T. T. Vu, “Physical layer secrecy performance over Rayleigh/Rician fading channels,” *in* International Conference on Advanced Technologies for Communications (ATC), Hanoi, Vietnam, Oct. 2014, pp. 113–118.

[8] S. Belmoubarik, G. Aniba, and B. Elgraini, “Secrecy capacity of a Nakagami-*m* fading channel in the presence of cooperative eavesdroppers,” *in* IEEE Mediterranean Microwave Symposium (MMS), Marrakech, Morocco, Dec. 2014, pp. 1–6.

[9] H. Lei, C. Gao, Y. Guo, and G. Pan, “On physical layer security over generalized gamma fading channels,” *IEEE Communications Letters*, vol. 19, no. 7, pp. 1257–1260, July 2015.

[10] L. Kong, H. Tran, and G. Kaddoum, “Performance analysis of physical layer security over α–μ fading channel,” *Electronics Letters*, vol. 52, no. 1, pp. 45–47, 2016.

[11] H. Lei, H. Zhang, I. S. Ansari, C. Gao., Y. Guo, G. Pan, and K. A. Qaraqe, “Performance analysis of physical layer security over generalized–*K* fading channels using a mixture gamma distribution,” *IEEE Communications Letters*, vol. 20, no. 2, pp. 408–411, Feb. 2016.

[12] N. Bhargav, S. L. Cotton, and D. E. Simmons, “Secrecy capacity analysis over κ–μ fading channels: Theory and applications,” *IEEE Transactions on Communications*, vol. 64, no. 7, pp. 3011–3024, July 2016.

[13] S. Iwata, T. Ohtsuki, and P. Y. Kam, “Secure outage probability over κ–μ fading channels,” *in* IEEE International Conference on Communications (ICC), Paris, France, May 2017, pp. 1–6.

[14] G. C. Alexandropoulos, and K. P. Peppas, “Secrecy outage analysis over correlated composite Nakagami–*m*/Gamma fading channels,” IEEE. Communications Letters, vol. 22. no. 1, pp. 77–80, Jan. 2018.

[15] L. Kong and G. Kaddoum, “On physical layer security over the Fisher-Snedecor $\mathcal{F}$ wiretap Fading Channels,” *IEEE Access*, vol. 6, pp. 39466–39472, 2018.

[16] L. Kong, S. Vuppala, and G. Kaddoum,

"Secrecy analysis of random MIMO wireless networks Over α–μ Fading Channels," *IEEE Transactions on Vehicular Technology*, vol. 67, no. 12, pp. 11654–11666, 2018.

[17] H. Zhao, Y. Liu, A. Sultan-Salem, and M.–S. Alouini, "A simple evaluation for the secrecy outage probability over generalized-K fading channels," *IEEE Communications Letters*, vol. 23, no. 9, pp. 1479-1483, 2019.

[18] D. Zwillinger, CRC Standard Mathematical Tables and Formulae, 31st ed. Boca Raton, FL: Chapman & Hall/CRC, 2003.

[19] Wolfram Research, Mathematica Edition: Version 8.0. Champaign, Illinois: Wolfram Research, Inc., 2010.

[20] F. Yilmaz, "On the relationships between average channel capacity, average bit error rate, outage probability and outage capacity over additive white Gaussian noise channels," *arXiv preprint* arXiv:1907. 06634, 2019.

[21] M. Abramowitz and I. A. Stegun, Handbook of Mathematical Functions with Formulas, Graphs, and Mathematical Tables, 9th ed. New York: Dover Publications, 1972

[22] F. Yilmaz, and M.-S. Alouini, "A unified MGF-based capacity analysis of diversity combiners over generalized fading channels," *IEEE Transactions on Communications*, vol. 60, no. 3, pp. 862-875, 2012.

[23] F. Yilmaz, and M.-S. Alouini, "Extended generalized-K (EGK): A new simple and general model for composite fading channels," arXiv preprint arXiv:1012.2598, 2010.

[24] F. Yilmaz, and M.-S. Alouini, "A new simple model for composite fading channels: Second order statistics and channel capacity," *in* International Symposium on Wireless Communication Systems (ISWCS), York, UK, Sep. 2010, pp. 676-680.

[25] M. A. Chaudhry and S. M. Zubair, On a Class of Incomplete Gamma Functions with Applications. Boca Raton-London-New York Washington, D.C.: Chapman & Hall/CRC, 2002.

[26] A. Kilbas and M. Saigo, H-Transforms: Theory and Applications. Boca Raton, FL: CRC Press LLC, 2004.

[27] A. M. Mathai, R. K. Saxena, and H. J. Haubold, The H-Function: Theory and Applications, 1st ed. Dordrecht, Heidelberg, London, New York: Springer Science, 2009.

[28] A. P. Prudnikov, Y. A. Brychkov, and O. I. Marichev, Integral and Series: Volume 3, More Special Functions. CRC Press Inc., 1990.

[29] N. C. Sagias, G. S. Tombras, and G. K. Karagiannidis, "New results for the Shannon channel capacity in generalized fading channels," *IEEE Communications Letters*, vol. 9, no. 2, pp. 97–99, Feb. 2005.